Bioorganic & Medicinal Chemistry Letters 21 (2011) 3648–3653

Contents lists available at ScienceDirect

Bioorganic & Medicinal Chemistry Letters

journal homepage: www.elsevier.com/locate/bmcl

Identification of 4H,6H-[2]benzoxepino[4,5-*c*][1,2]oxazoles as novel squalene synthase inhibitors

Nils Griebenow [a,*], Anja Buchmueller [b], Peter Kolkhof [b], Jens Schamberger [a], Hilmar Bischoff [b]

[a] Bayer Pharma AG, Global Drug Discovery, Medicinal Chemistry Wuppertal, Building 460, D-42096 Wuppertal, Germany
[b] Bayer Pharma AG, Global Drug Discovery, Cardiology Research, Building 500, D-42096 Wuppertal, Germany

ARTICLE INFO

Article history:
Received 19 March 2011
Revised 18 April 2011
Accepted 20 April 2011
Available online 29 April 2011

Keywords:
Squalene synthase inhibitor
SAR
Atherosclerosis
4H,6H-[2]Benzoxepino[4,5-*c*][1,2]oxazole

ABSTRACT

Novel squalene synthase inhibitors are disclosed. The design, synthesis, SAR and pharmacological profile of the compounds are discussed.

A large number of epidemiological studies have shown a causal connection between dyslipidemias and cardiovascular disorders. Elevated plasma cholesterol, mainly LDL-cholesterol, is one of the highest risk factors for cardiovascular disorders, such as atherosclerosis.[1] This relates both to an isolated hypercholesterolemia and to hypercholesterolemia combined with elevated plasma triglycerides or low plasma HDL-cholesterol. The standard of care in hypercholesterolemia is the use of statins which can reduce mortality and morbidity among patients with cardiovascular disorders. Statins block one of the key enzymes, HMG-CoA reductase, in the cholesterol biosynthesis pathway which leads to a compensatory up-regulation of hepatic LDL-receptors.

However, since about half of patients treated with statins do not reach target LDL levels due to efficacy limitations or even non-response, additional lipid lowering therapies are necessary. Squalene synthase (EC 2.5.1.21) catalyzes the conversion of farnesyl pyrophosphate into squalene by reductive condensation. This is another crucial step in cholesterol biosynthesis. Whereas HMG-CoA reductase inhibitors also block the synthesis of essential non-sterol isoprenoids like farnesyl pyrophosphate which are also of importance for other cellular metabolic pathways and reactions, squalene serves as the exclusive precursor for cholesterol. Inhibition of squalene synthase leads directly to a reduction in cholesterol biosynthesis and thus to a fall in plasma cholesterol levels. It has already been shown in animal models and in humans that plasma LDL-cholesterol and triglycerides are lowered by squalene synthase inhibitors. Substances which have a cholesterol or combined cholesterol and triglyceride lowering effect ought therefore

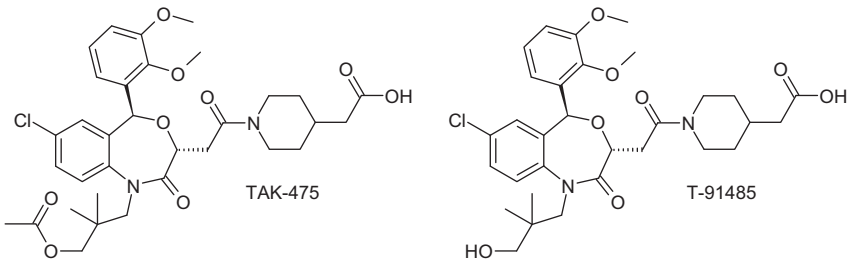

Figure 1. Chemical structure of lapaquistat acetate (TAK-475) and its active metabolite (T-91485).

* Corresponding author. Tel.: +49 202 36 5866.
E-mail addresses: nils.griebenow@bayer.com, nils.griebenow@bayerhealthcare.com (N. Griebenow).

0960-894X/$ - see front matter © 2011 Elsevier Ltd. All rights reserved.
doi:10.1016/j.bmcl.2011.04.092

to be suitable for the treatment and prevention of cardiovascular disorders.[1c]

Herein, we describe a structure based design approach to a novel class of squalene synthase inhibitors. Starting point for our investigations was the most advanced squalene synthase inhibitor lapaquistat acetate (TAK-475), which is so far the only squalene synthase inhibitor progressed into phase III clinical trials (Fig. 1).[2]

Contemplating the backbone of lapaquistat acetate,[3] our design plan was to replace the central amide group by an amide bioisostere, such as a five membered heterocyclic moiety.[4] In detail, we envisioned to replace the amide by an isoxazole,[4] whereby the nitrogen of the heterocycle should be able to act as a hydrogen bond acceptor like the carbonyl group of the amide (Fig. 2).[5]

A good match of electronic and geometrical properties was supported by molecular modeling (Fig. 3).[6] It was proposed that the introduction of this bioisosteric group would improve pharmacological and physicochemical properties, because such a scaffold has a reduced number of rotational bonds and the presumably metabolic labile amide bond is replaced.

Further insight into the role of the amide carbonyl was gained by analysis of the published X-ray crystal structure of squalene synthase by Pandit et al.[7] The co-crystallized ligand CP-320473 exhibits the same core structure as TAK-475 (Fig. 4). The crystal structure revealed a water mediated hydrogen bond between the carbonyl group of the amide and Asn 215. Virtual docking of **13d** confirmed that this water bridge could well be established by the benzoxepino-oxazole scaffold (Fig. 5).[8]

Inspired by a report of Moore et al.[9] describing the synthesis of trisubstituted isoxazole 4-boronates with high levels of regiocontrol (Scheme 1), we considered isoxazole **1** as a suitable key building block for the synthesis of the projected benzoxepino-oxazole scaffold.

In detail, such a building block should allow for facile C–C bond formation between an aromatic moiety and the isoxazole via Suzuki cross-coupling, as well as for the further elaboration of the dimethyl acetal group towards the required acrylate for ring closure reaction (see Scheme 2).

Thus isoxazole **1** was synthesized as outline in Scheme 3.[10] Initially, glyoxal dimethyl acetal (**6**) was reacted with hydoxylamine to provide the aldoxime, which was converted into the *N*-hydroxyimidoyl chloride **2** upon treatment with *N*-chloro-succinimide. In parallel, alkyne **7** was transformed into the alkynylboronate **3** via deprotonation with *n*-butyl lithium followed by reaction with 2-isopropoxy-4,4,5,5-tetramethyl-1,3,2-dioxaborolane. Finally [2+3] cycloaddition reaction of **2** and **3** yielded the target isoxazole **1** as a single regioisomer.[11] Instead of the typical Huisgen-protocol,[12] the nitrile oxide from **2** was generated with potassium bicarbonate in dimethoxyethane according to the method of Moore et al.[9]

Because of its low basicity and solubility in dimethoxyethane, potassium bicarbonate permits the slow generation of the nitrile

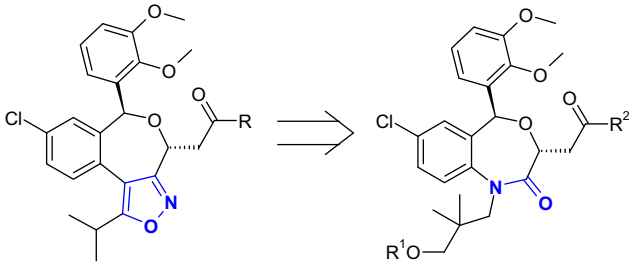

Figure 2. Design approach yielding the benzoxepino-oxazole scaffold derived from TAK-475 and T-91485.

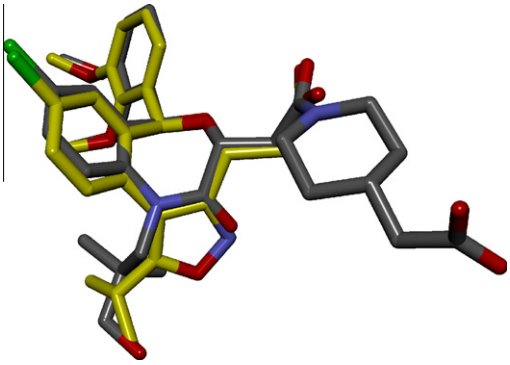

Figure 3. Superimposition of T-91485 (gray) and **13d** (yellow).

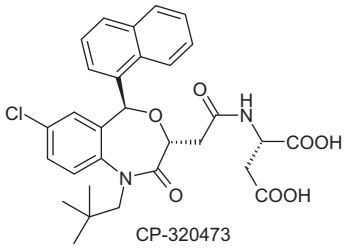

Figure 4. Structure of CP-320473, which was co-crystallized with squalene synthase (PDB entry code 1EZF).

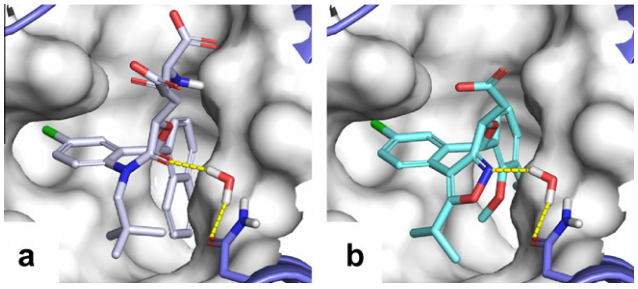

Figure 5. (a) X-ray crystal structure of squalene synthase in complex with inhibitor CP-320473; (b) Best virtual docking pose of **13d**.

oxide to minimize unwanted nitrile oxide dimerization. However the yield of the cycloaddition remains low to moderate.[13] The second key intermediate **5** was built-up starting from commercial 2-amino-5-chloro-benzoic acid (**8**) as shown in Scheme 4.

Anthranilic acid **8** was converted to benzoxazinone **9** upon treatment with acetic anhydride under refluxing conditions. Addition of lithiated 1,2-dimethoxybenzene to **9** and refluxing in hydrochloric acid yielded **10**. Conversion of the amino functionality of **10** via anhydrous diazotiziation followed by treatment with sodium iodide in acetone afforded the iodo-compound **5**.[9]

Having both key intermediates in hand we investigated the further elaboration to the benzoxepino-oxazole scaffold as outlined in Scheme 2. Initially building blocks **1** and **5** were reacted in a Suzuki cross-coupling reaction[14] to the biaryl compound **11** (Scheme 5). Elaboration of the acetal **11** to the acrylate **4** was performed via treatment with aq HCl followed by Wittig-olefination[15] of the formed aldehyde with ethoxy-carbonylmethyltriphenylphosphorane. Selective reduction of the ketone moiety of **4** and subsequent cyclization of the alcohol via 1,4-addition upon treatment with Schwesinger phosphazene base *tert*-Bu-P_2[16] yielded the

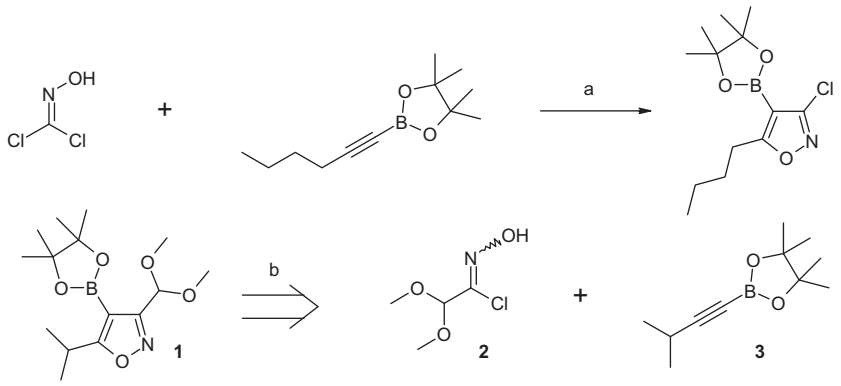

Scheme 1. Reagents and conditions: (a) $KHCO_3$, DME, 16 h, 50 °C (44%). For details see Moore et al. Ref. 9 (b) Proposed synthetic access to target intermediate **1**.

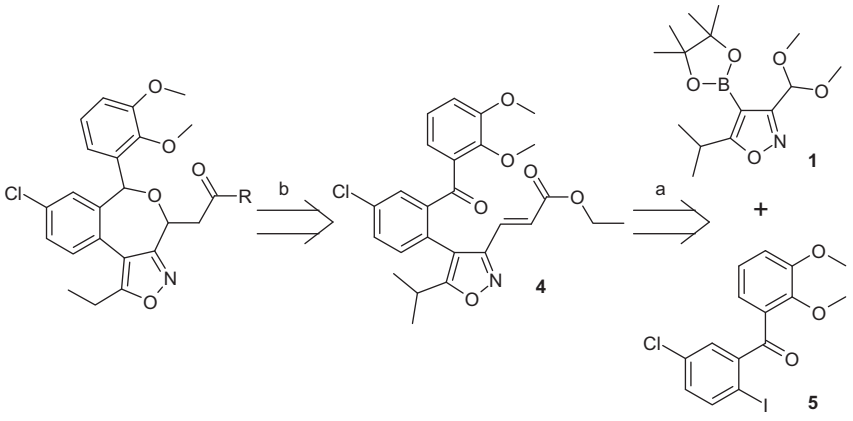

Scheme 2. (a) Retrosynthetic approach: Suzuki cross-coupling of building blocks **1** and **5** and further elaboration of the dimethyl acetal to the acrylate **4**; (b) Selective reduction at the ketone of intermediate **4** and cyclization of the formed alcohol by 1,4-addition to the acrylate.

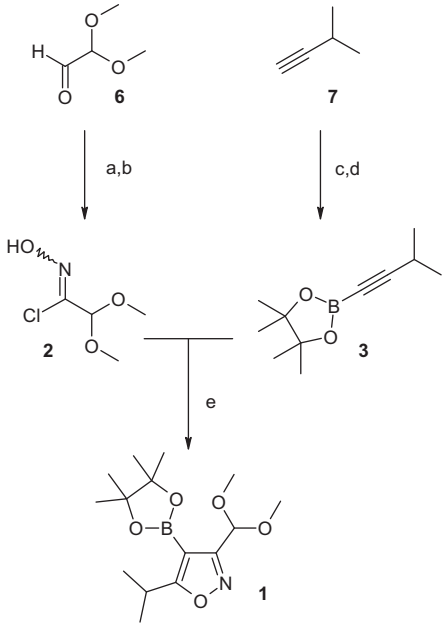

Scheme 3. (a) Glyoxal dimethylacetal (45% in *tert*-butyl methyl ether), hydroxylamine (prepared from hydroxylamine hydrochloride and NaOMe), methanol, rt, 16 h; (b) DMF, *N*-chloro-succinimide, 3 h, rt (28% over two steps); (c) *n*-BuLi, THF, −78 °C, 30 min; (d) 2-isopropoxy-4,4,5,5-tetramethyl-1,3,2-dioxaborolane, 2 h, −78 °C (88%); (e) $KHCO_3$, DME, 50 °C, 56 h (17%).

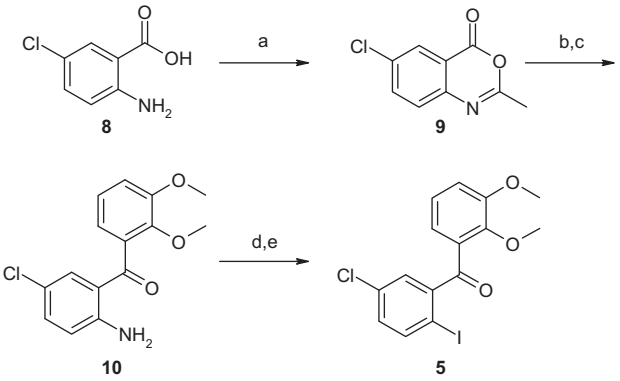

Scheme 4. Reagents and conditions: (a) Ac_2O, reflux, 2 h (83%); (b) 1,2-dimethoxybenzene, THF, *n*-BuLi, 0 °C, 1 h; (c) concn aq HCl, EtOH, H_2O, reflux, 3 h (47% over two steps); (c) THF, boron trifluoride–diethyl ether complex, isoamyl nitrite, −10 °C, 30 min; (d) NaI, acetone, rt, 20 min (41% over two steps).

benzoxepino-oxazole **12** as a mixture of diastereomers (ds = 58:42). Saponification followed by separation of the four stereoisomers by chiral HPLC provided the isolated isomers **13a–d**.[10] The IC_{50} values of the isomers **13a–d** were determined by a biochemical assay measuring the conversion of farnesyl pyrophosphate to squalene by squalene synthase.[17] The absolute stereochemistry of the benzoxepino-oxazole **13d** was assigned by

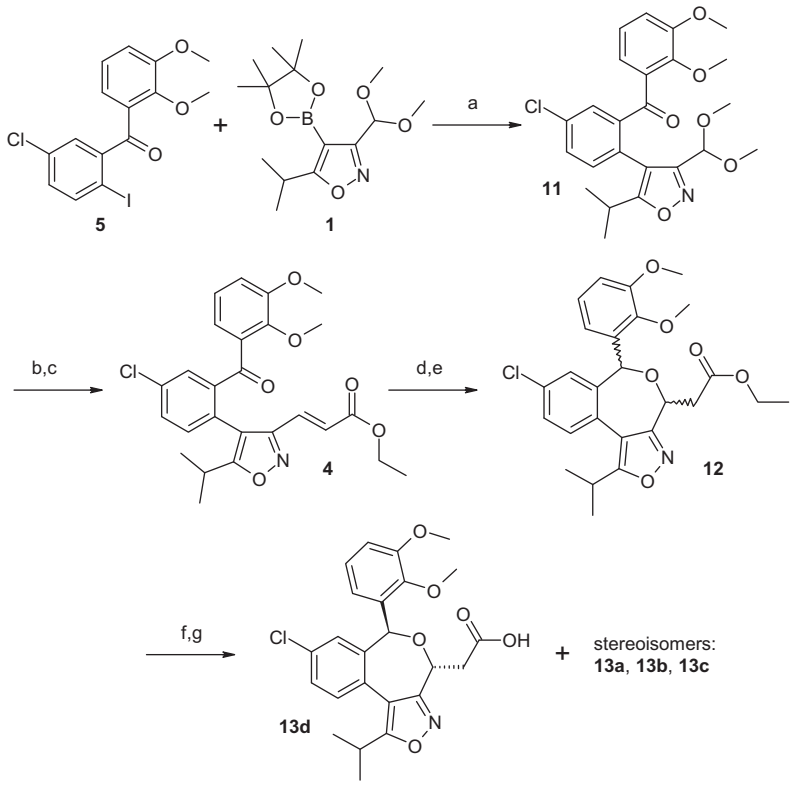

Scheme 5. Reagents and conditions: (a) K_3PO_4, dioxane [1,1'-bis(diphenylphosphino)-ferrocene]di-chloropalladium(II) (1:1 complex with DCM), 85 °C, 72 h (42%); (b) THF, 10% aq HCl, reflux, 42 h; (c) ethoxy-carbonylmethyltriphenylphosphorane, DCM, rt, 16 h (72% over two steps); (d) lithium tri(*tert*-butyloxy)aluminum hydride THF, 0 °C, 2 h; (e) 1-*tert*-butyl-2,2,4,4,4-pentakis(dimethylamino)-2^5,4^5-catenodi(phosphazene) (phosphazene base *tert*-Bu-P_2), THF, 0 °C, 1 h, (36%, mixture of two couples of diastereomers, dr = 58:42); (f) dioxane, water, concn HCl, 80 °C, 19 h (51%); (g) separation of the four stereoisomers by preparative HPLC on a chiral phase (**13d**: 14%).

Table 1
SAR of the benzoxepino-oxazoles

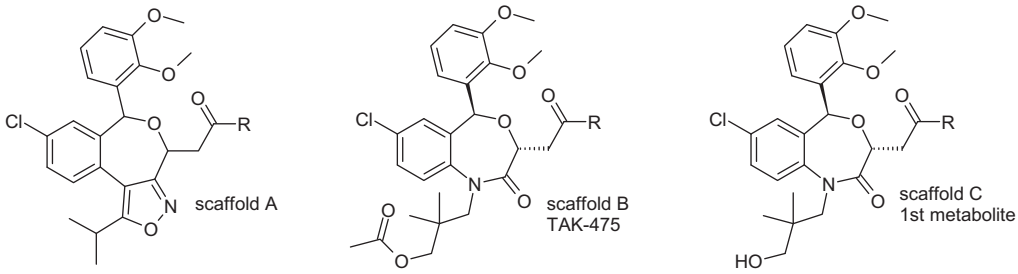

Compound[a]	Scaffold	Isomer	R	IC_{50}[b] (nM)	HLM[c] (%)	Sterol biosynthesis[d] (%)	
						3 mg/kg po	1 mg/kg po
13a	A	1[e]	OH	1420	nd	nd	nd
13b	A	2[e]	OH	5500	nd	nd	nd
13c	A	3[e]	OH	169	64	31	nd
13d	A	4[e]	OH	56	100	58	nd
14d	A	4	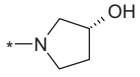	162	nd	nd	nd
15d	A	4	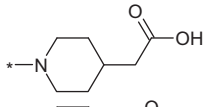	131	91	80	nd
16d	A	4	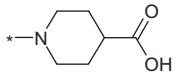	112	98	79	71
TAK-475	B	—	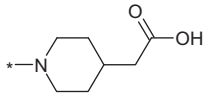	213	7	73	59

(*continued on next page*)

Table 1 (*continued*)

Compound[a]	Scaffold	Isomer	R	IC_{50}[b] (nM)	HLM[c] (%)	Sterol biosynthesis[d] (%)	
						3 mg/kg po	1 mg/kg po
16	C	–	OH	223	nd	nd	nd
T-91485	C	–	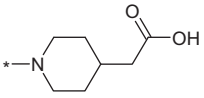	260	37	nd	nd

[a] For experimental data of compounds **13a–d**. **14d**, **15d** and **16d** see Ref. 10.
[b] Values are means of three experiments. For a detailed description of the biochemical assay see Ref. 17.
[c] Human liver microsomal stability, % compound remaining after 60 min.
[d] Inhibition of sterol biosynthesis in % (in vivo). For details see Ref. 19.
[e] ^{1}H NMR spectra indicated that **13a** and **13d** as well as **13b** and **13c** are pairs of enantiomers.

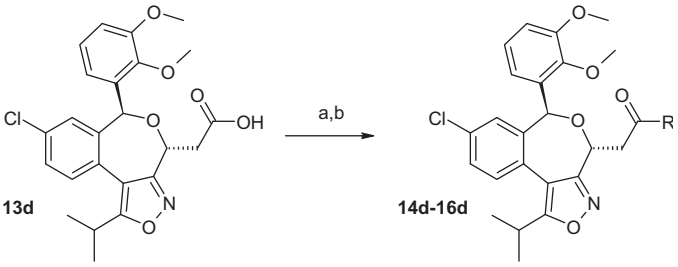

Scheme 6. Reagents and conditions: (a) Ethyl piperidine-4-carboxylate or ethyl piperidin-4-ylacetate or (3R)-pyrrolidin-3-ol, PyBOP, DIEA, rt, 16 h. (b) In case of amines bearing an ester group: dioxane, water, concn aq HCl, 60 °C, 16 h.

analogy to the stereoselective inhibitory potencies of 4,1-benzoxazepine derivatives (Table 1).[3b]

The stereoisomer **13d** was elaborated further at the carboxylic acid to the amides **14d–16d** as outlined in Scheme 6. Because of the previously established structure activity relationship,[18] we considered only small variations at the carboxylic acid. Amide formation was accomplished under standard coupling conditions (PyBOP, DIEA).

Surprisingly, all the amides **14d–16d** showed a higher in vitro potency compared to lapaquistat acetate (Table 1). Compounds **13d**, **15d** and **16d** were progressed further to in vivo animal studies. Inhibition of hepatic cholesterol biosynthesis was investigated in NMRI-mice.

After po administration of 3 mg/kg, the compounds **13d**, **15d** and **16d** showed a reduction in sterol biosynthesis of 58%, 80% and 79% respectively (Table 1).[19]

The best match of in vitro potency and microsomal stability combined with a pronounced reduction in sterol biosynthesis was displayed by compound **16d**.[20] Thus **16d**, was investigated at lower dosage in NMRI-mice (1 mg/ kg po) showing a reduction in sterol biosynthesis of 71%.

In conclusion, we have identified a novel series of substituted benzoxepino-oxazoles which have a superior profile compared to lapaquistat acetate (TAK-475) and its active metabolite T-91485, regarding in vitro potency and microsomal stability as well as reduction of sterol biosynthesis. Further pharmacological data of **16d** will be reported in due course.

Acknowledgements

We thank our Analytical Chemistry colleagues for structure and purity determination. In addition, we are grateful to Dr. Klemens Lustig for providing microsomal stability data, and Dr. Stuart Ince and Dr. Hartmut Schirok for critical reading of the manuscript and helpful discussions.

References and notes

1. (a) Carpender, K. I.; Taylor, S. E.; Ballantine, J. A.; Fussell, B.; Halliwell, B.; Mitchinson, M. J. *Biochim. Biophys. Acta* **1993**, *1167*, 121; (b) Brown, A. J.; Mander, E. L.; Gelissen, I. C.; Kritharides, L.; Dean, R. T.; Jessup, W. *J. Lipid Res.* **2000**, *41*, 226; (c) Kourounakis, A. P.; Charitos, C.; Rekka, E. A.; Kourounakis, P. N. *J. Med. Chem.* **2008**, *51*, 5861.
2. (a) Burnett, J. *Curr. Opin. Investig. Drugs.* **2006**, *7*, 850; (b) Seiki, S.; Frishman, W. H. *Cardiol. Rev.* **2009**, *17*, 70; (c) Elsayed, R. K.; Evans, J. D. *Expert Opin. Emerging Drugs* **2008**, *13*, 309.
3. (a) Miki, T.; Kori, M.; Fujishima, A.; Mabuchi, H.; Tozawa, R.; Nakamura, M.; Sugiyama, Y.; Yukimasa, H. *Bioorg. Med. Chem.* **2002**, *10*, 385; (b) Miki, T.; Kori, M.; Mabuchi, H.; Banno, H.; Tozawa, R.; Nakamura, M.; Itokawa, S.; Sugiyama, Y.; Yukimasa, H. *Bioorg. Med. Chem.* **2002**, *10*, 401.
4. (a) Pevarello, P.; Amici, R.; Brasca, M. G.; Villa, M.; Varasi, M. *Targets in Heterocycl. Syst.* **1999**, *3*, 301; (b) Mogensen, J. P.; Roberts, S. M.; Bowler, A. N.; Thomsen, C.; Knutsen, L. J. S. *Bioorg. Med. Chem. Lett.* **1998**, *8*, 1767.
5. (a) Nobeli, I.; Price, S. L.; Lommerse, J. P. M.; Taylor, R. *J. Comput. Chem.* **1997**, *18*, 2060; (b) Böhm, H.-J.; Klebe, G.; Brode, S.; Hesse, U. *Chem. Eur. J.* **1996**, *2*, 1509; (c) Liu, G.; Xin, Z.; Pei, Z.; Hajduk, P. J.; Abad-Zapatero, C.; Hutchins, C. W.; Zhao, H.; Lubben, T. H.; Ballaron, S. J.; Haasch, D. L.; Kaszubska, W.; Rondinone, C. M.; Trevillyan, J. M.; Jirousek, M. R. *J. Med. Chem.* **2003**, *46*, 4232; (d) Sharp, S. Y.; Prodromou, C.; Boxall, K.; Powers, M. V.; Holmes, J. L.; Box, G.; Matthews, T. P.; Cheung, K.-M. J.; Kalusa, A.; James, K.; Hayes, A.; Hardcastle, A.; Dymock, B.; Brough, P. A.; Barril, X.; Cansfield, J. E.; Wright, L.; Surgenor, A.; Foloppe, N.; Hubbard, R. E.; Aherne, W.; Pearl, L.; Jones, K.; McDonald, E.; Raynaud, F.; Eccles, S.; Drysdale, M.; Workman, P. *Mol. Cancer Ther.* **2007**, *6*, 1198.
6. (a) Flexible structural alignment was carried out using the program Surflex Sim provided with SYBYL-X 1.2 (Tripos Int., St. Louis, MO, USA).; (b) Jain, A. N. J. *Comput.-Aided Mol. Des.* **2000**, *14*, 199; Structures were optimized prior to alignment using the MMFF94s force field, supplied with SYBYL-X 1.2, see (c) Halgren, T. *J. Comp. Chem.* **1999**, *20*, 720.
7. Protein Data Bank, Research Collaboratory for Structural Bioinformatics, Rutgers University, New Brunswick, NJ (http://www.rcsb.org) with reference code **1EZF**. See: Pandit, J.; Danley, D. E.; Schulte, G. K.; Mazzalupo, S. *J. Biol. Chem.* **2000**, *275*, 30610.
8. Docking studies were carried out employing the Schrödinger suite of programs. The X-ray crystal structure **1EZF** was used as a glide receptor grid after protein preparation. The water forming a bridge to ASN 215 was included into the receptor grid. Ligands were optimized before docking via the ligprep routine. Docking was carried out in SP and XP mode with similar results. Figures were prepared with PyMol.; (b) Glide, version 5.6, Schrödinger, LLC, New York, NY, 2010.; (c) LigPrep, version 2.4, Schrödinger, LLC, New York, NY, 2010.; (d) The PyMOL Molecular Graphics System, Version 1.3, Schrödinger, LLC.
9. (a) Moore, J. E.; Davies, M. W.; Goodenough, K. M.; Wybrow, R. A. J.; York, M.; Johnson, C. N.; Harrity, J. P. A. *Tetrahedron* **2005**, *61*, 6707; (b) Moore, J. E.; Goodenough, K. M.; Spinks, D.; Harrity, J. P. A. *Synlett* **2002**, 2071.
10. For experimental details and characterization of the compounds see: (a) Griebenow, N.; Buchmueller, A.; Kolkhof, P.; Bischoff, H. PCT Int. Appl., WO 2008003424, 2008. (b) Griebenow, N.; Buchmueller, A.; Kolkhof, P.; Bischoff, H. US 2010016299, 2010.
11. The geometry of the isoxazole **1** was reasoned from the subsequent synthesis steps providing the 4,1-benzoxazepine scaffold. The regioisomeric 3-(dimethoxymethyl)-4-isopropyl-5-(4,4,5,5-tetramethyl-1,3,2-dioxaborolan-2-yl)-1,2-oxazole will not yield such a cyclization pruduct.
12. Generation of nitrile oxides from N-hydroxyimidoyl chlorides by slow addition of triethylamine, where the stationary concentration of nitrile oxide is kept low to avoid dimerization: Huisgen, R. *Angew. Chem., Int. Ed.* **1963**, *2*, 565.
13. Yields were low due to dimerization of the formed nitrile oxide and protodeborylation of the product.
14. For comprehensive reviews, see: (a) Suzuki, A. *Pure Appl. Chem.* **1994**, *66*, 213; (b) Miyaura, N.; Suzuki, A. *Chem. Rev.* **1995**, *95*, 2457; (c) Bellina, F.; Carpita, A.; Rossi, R. *Synthesis* **2004**, *15*, 2419.
15. Wittig, G.; Schöllkopf, U. *Chem. Ber.* **1954**, *87*, 1318.
16. Schwesinger, R.; Schlemper, H. *Angew. Chem., Int. Ed.* **1987**, *26*, 1167.

17. Squalene synthase catalyses the reductive condensation of farnesyl pyrophosphate to squalene during cholesterol biosynthesis. Turnover of *trans,trans*-[1-^{3}H]-farnesyl pyrophosphate to [^{3}H]-squalene by squalene synthase was determined under the following conditions: 0.03 μg recombinant SQS, 1 mM NADPH, 5 mM DTT, 10% PBS, 10 mM sodium fluoride, 0.5 mM $MgCl_2$, pH 7.5. Test compounds were dissolved in DMSO and added in defined concentrations. The assay was started by adding farnesyl pyrophosphate (final conc. 5 μM) and 0.2 nM *trans,trans*-[1-^{3}H]-farnesyl pyrophosphate and incubated for 10 min at 37 °C. Subsequently, 100 μl solution was extracted with 200 μl chloroform, 200 μl methanol and 60 μl 5 N sodium hydroxide and adjusted to 2 mM squalene. An aliquot of the organic phase was mixed with scintillation fluid and measured for β-emission.
18. Griebenow, N.; Flessner, T.; Buchmueller, A.; Raabe, M.; Bischoff, H.; Kolkhof, P. *Bioorg. Med. Chem. Lett.* **2011**, *21*, 2554.
19. The compounds were administered orally to NMRI-mice ($n = 8$) 1 h before monitoring of the cholesterol synthesis started. Biosynthesis of [^{14}C]-labeled cholesterol and its precursors was monitored after ip application of [^{14}C]-mevalonolactone. One hour after mevalonolactone application, livers were removed and the amount of hepatic [^{14}C]-cholesterol synthesis was determined after sterol extraction by liquid scintillation counting. See also: Duncan, I. W.; Culbreth, P. H.; Burtis, C. A. *J. Chromatogr.* **1979**, *162*, 281.
20. *Experimental data for* **16d**: ^{1}H NMR (400 MHz, $CDCl_3$): $\delta = 1.36$ (d, $J = 6.9$, 3H), 1.48–1.98 (m, 4H), 1.51 (d, $J = 6.9$, 3H), 2.49–2.58 (m, 1H), 2.79–3.02 (m, 2H), 3.07–3.20 (m, 2H), 3.44 (s, 3H), 3.46 (sept, $J = 6.9$, 1H), 3.84–3.89 (m, 4H), 4.32–4.46 (m, 1H), 5.23–5.37 (m, 1H), 5.87 (s, 1H), 6.71–6.73 (m, 1H), 6.91–6.95 (m, 1H), 7.14–7.18 (m, 1H), 7.24–7.35 (m, 3H). LC/MS (for instrumentation and conditions see Ref. 21): 2.59 min, 100% (214 nm), $m/z = 569$ $[M+H]^+$.
21. Intrument: Micromass Quattro LCZ with HPLC Agilent Series 1100; column: Phenomenex Synergi 2 μ Hydro-RP Mercury, 20 × 4 mm; eluent A: 1 l water + 0.5 ml 50% formic acid; eluent B: 1 l acetonirile + 0.5 ml 50% formic acid; gradient: 0.0 min 90% A→2.5 min 30% A→3.0 min 5% A→4.5 min 5% A; flow rate: 0.0 min 1 ml/min→2.5 min/3.0 min/4.5 min 2 ml/min; oven: 50 °C; UV detection: 208–400 nm.